JOURNAL OF MATERIALS SCIENCE 28 (1993) 3962–3968

Piezoelectric tubes and tubular composites for actuator and sensor applications

Q. M. ZHANG, H. WANG, L. E. CROSS
Materials Research Laboratory, The Pennsylvania State University, University Park, PA 16802, USA

Piezoelectric actuators and sensors made with a tubular structure can provide a great agility of effective response in the radial direction. For a radially poled piezoelectric tube, the effective piezoelectric constant in that direction can be tuned to be positive, zero or negative by varying the ratio of the outer radius (R_0) to the inner radius (r_0) of the tube. For a suitable ratio of R_0/r_0, this effective constant can also be changed in sign or set to zero by adjusting the d.c. bias field level for tubes made of electrostrictive materials. Therefore, one can make a piezoelectric transducer with all the effective piezoelectric tensile constants having the same sign. End-capped thin-walled tubes also exhibit an exceptionally high hydrostatic response, and the small size of the tubular structure makes it very suitable for integration into a 1–3 composite which possesses low acoustic impedance and high hydrostatic response.

1. Introduction

The recent advance in adaptive materials and structures has put increasing demands on new materials and material structures to broaden the range of material properties provided by conventional materials [1, 2]. The novel concept of piezocomposites is one such example which combines two or more materials with complementary properties to expand the effective properties of the composite beyond those of each individual component [3, 4]. With the existing materials, by structure modifications, one can also greatly improve the performance of devices. In this paper, we will examine the effective piezoelectric properties of a tubular structure and its composites formed from arrays of such tubes for both actuating and sensing applications. For a radially poled ceramic tube, the competition between the piezoelectric d_{33} effect and d_{31} effect in the radial direction provides a convenient way to adjust the effective piezoelectric properties in that direction by changes in the tube radii. The small thickness of a thin-walled tube also makes it practical to use field-biased electrostrictive materials for actuators and sensors, since only a low terminal d.c. voltage is required to produce substantial piezoelectric activities in materials with this geometry.

2. Piezoelectric response of a tube under an electric field

When a radially poled tube is subjected to an electric field along the radial direction, on the average, the strain in the axial direction equals $d_{31}E_m$, where d_{31} is the linear piezoelectric constant and E_m is the average field in the material. The dimensional change in the radial direction, however, is complicated. In this section, the solution of the elastic equation for the tubular structure under an electric field will be presented. It will be shown that with the same applied electric field, the outer diameter (o.d.) (or the inner diameter (i.d.)) of the tube can either expand or contract depending on the ratio of the o.d. to i.d. of the tube. This phenomenon is a direct consequence of competition between the piezoelectric d_{33} and d_{31} effects, which have opposite sign in producing the change in the tube o.d. under an electric field.

For a tubular structure, it is convenient to use the cylindrical polar coordinate system, as shown in Fig. 1, in the analysis of the strain response of the sample under an electric field. The symmetry of the problem requires that the ϕ component of the displacement field $u_\phi = 0$. For a thin-walled tube one can neglect the coupling terms containing both r and z in the displacements field $\boldsymbol{u}$ and assume $\boldsymbol{u} = u_r(r)\hat{r} + u_z(z)\hat{z}$. Under this approximation, the non-zero strain components are

$$u_{rr} = \frac{\partial u_r}{\partial r} \qquad u_{\phi\phi} = \frac{u_r}{r} \qquad u_{zz} = \frac{\partial u_z}{\partial z}$$

The constitutive relations for the tube, therefore, are

$$\begin{aligned} T_z &= c_{11}u_{zz} + c_{12}u_{\phi\phi} + c_{12}u_{rr} - e_{31}E \\ T_r &= c_{11}u_{rr} + c_{12}u_{\phi\phi} + c_{12}u_{zz} - e_{33}E \\ T_\phi &= c_{12}u_{zz} + c_{11}u_{\phi\phi} + c_{12}u_{rr} - e_{31}E \end{aligned} \quad (1)$$

where T_z, T_r and T_ϕ are the stress components in the three directions, c_{ij} is the elastic stiffness constant, e_{ij} is the piezoelectric stress constant, and E is the applied electric field on the tube wall along the r direction. It is well known that the electric field is not a constant inside the tube wall and with a total voltage V applied on the tube, $E = V/r\ln(R_0/r_0)$ $(r_0 \leq r \leq R_0)$. In writing down Equation 1, we also made the approximation that the tube is isotropic elastically to simplify the analysis. The non-isotropic case will be addressed in

0022–2461

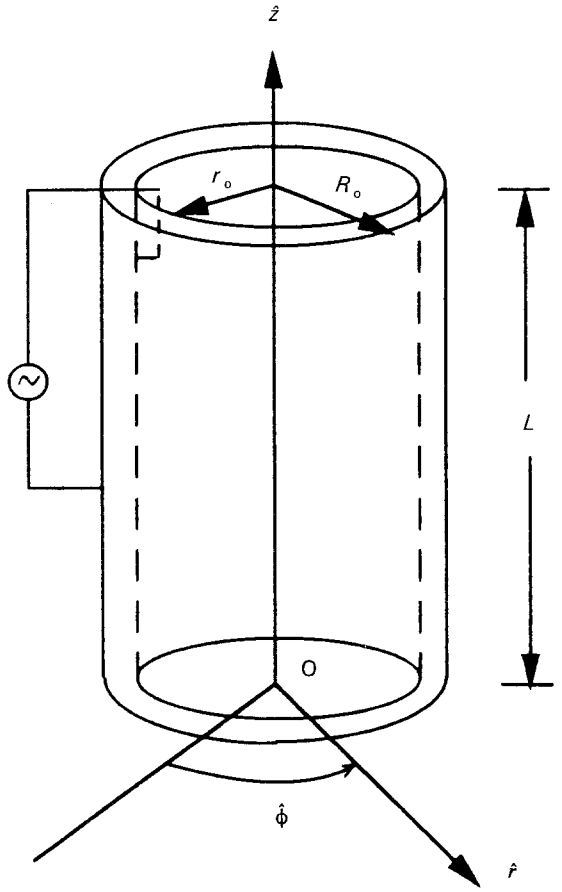

Figure 1 Schematic drawing of a radially poled ceramic tube with outer radius R_0, inner radius r_0 and total length L. The electric field is applied on the tube wall along the radial direction.

the next section when we discuss the hydrostatic response of end-capped tubes. Both the experimental results which will be presented later in this section and the analysis in the next section show that the errors due to the isotropic approximation are not significant.

Making use of the constitutive Equation 1 and the static equilibrium condition, we can derive the basic elastic equations for this problem [5]:

$$\frac{\partial}{\partial r}\left[\frac{1}{r}\left(\frac{\partial(ru_r)}{\partial r}\right)\right] = -\left(\frac{e_{31}E}{r}\right)\frac{s_{11}(1+\sigma)(1-2\sigma)}{1-\sigma}$$

$$\frac{\partial u_z}{\partial z} = \text{constant} \tag{2}$$

where σ is Poisson's ratio and s_{11} is the elastic compliance. The solutions to Equation 2 are

$$u_r = ar + \frac{b}{r} + \left(\frac{e_{31}V}{\ln\rho}\right)\frac{s_{11}(1+\sigma)(1-2\sigma)}{1-\sigma}$$

$$u_z = cz \tag{3}$$

where $\rho = R_0/r_0$. a, b and c are the integration constants which can be determined from the boundary conditions: $u_{zz} = d_{31}E_m$, where E_m is the average electric field in the tube and $E_m = 2V/[(R_0 + r_0) \times \ln(R_0/r_0)]$; at $r = R_0$ and r_0 there is no external stress on the tube wall, which implies $T_r = 0$ at these two boundaries. Substituting Equation 3 into Equation 1 and using the boundary conditions, one can get

$$a = E_m\frac{(1-2\sigma)d_{33} - \sigma d_{31}}{2(1-\sigma)}$$

$$b = -R_0r_0E_m\frac{d_{33} + \sigma d_{31}}{2(1-\sigma)}$$

$$c = d_{31}E_m \tag{4}$$

All the strain components for the tube can be obtained from Equations 3 and 4. Here we are more interested in finding out how the tube outer diameter changes with applied electric field as the ratio R_0/r_0 varies since in most of the applications, this is the quantity of interest. Substituting a and b in Equation 4 into the expression for u_r and setting $r = R_0$ yields the displacement of the tube outer wall $u_r(R_0)$:

$$u_r(R_0) = E_m\frac{(R_0 + r_0)d_{31} + (R_0 - r_0)d_{33}}{2}$$

This equation reveals that $u_r(R_0)$ can be changed from positive to zero, and to negative, by varying the ratio of R_0/r_0.

To illustrate the advantage of using thin-walled tubes for actuator applications, one can compare the piezoelectric response of a tube discussed here with a rod of radius R_0 and length L subjected to the same applied voltage V. For the rod, the field is applied along the axial direction and $u_{zz} = d_{33}V/L$ and $u_{rr} = d_{31}V/L$. For the tube sample, one can equivalently introduce the quantity u_r/R_0 as the effective strain in the radial direction:

$$\frac{u_r(R_0)}{R_0} = E_m\frac{[1 + (r_0/R_0)]d_{31} + [1 - (r_0/R_0)]d_{33}}{2} \tag{5}$$

Similar to a rod sample, we introduce the effective piezoelectric constants for the tube as if it were a rod poled axially:

$$u_{zz} = d_{33}^{\text{eff}}\frac{V}{L} \qquad \frac{u_r}{R_0} = d_{31}^{\text{eff}}\frac{V}{L} \tag{6}$$

where L is the axial length of the tube and V is the voltage applied on the tube wall. From $u_{zz} = d_{31}E_m$ and Equation 5, the effective piezoelectric constants can be deduced as

$$d_{33}^{\text{eff}} = d_{31}\frac{2L}{(R_0 + r_0)\ln(R_0/r_0)}$$

$$d_{31}^{\text{eff}} = \frac{L}{(R_0 + r_0)\ln(R_0/r_0)} \times \left[\left(1 + \frac{r_0}{R_0}\right)d_{31} + \left(1 - \frac{r_0}{R_0}\right)d_{33}\right] \tag{7}$$

For thin-walled tubes with L much larger than R_0, which is the case in most of the applications, both d_{33}^{eff} and d_{31}^{eff} can be exceptionally large. This demonstrates that the tubular structure has great advantage over the regular ceramic rod for actuator application. Besides that, by choosing $[1 + (r_0/R_0)]|d_{31}| > [1 - (r_0/R_0)]|d_{33}|$, the effective d_{33} and d_{31} of the tube will have the same sign. By adjusting the ratio

R_0/r_0, one can also continuously vary d_{31}^{eff} of the tube from positive to zero and to negative.

To compare with the theoretical prediction, the displacement field $u_r(R_0)$ and u_{zz} of a radially poled PZT-5 tube were measured using a double-beam laser dilatometer [6]. The ceramic tubes used were manufactured by Morgon Matroc, Inc., Vernitron Divisions, with $R_0 = 0.635$ mm and $r_0 = 0.381$ mm. From the data acquired and using Equations 3, 4 and 5, we got $d_{33} = 289$ pC N^{-1} and $d_{31} = -141.3$ pC N^{-1} for the tube material. For most of the commercially available PZT materials, the ratio d_{33}/d_{31} ranges from 2.15 to 2.3 [7]. The measured ratio here ($d_{33}/d_{31} = 2.05$) is slightly below that range which we believe is the result of the approximations used in the derivation. The effective piezoelectric constants defined in Equation 6 for the tube, therefore, are $d_{33}^{\text{eff}} = -8180$ pC N^{-1} and $d_{31}^{\text{eff}} = -3220.5$ pC N^{-1}; the two coefficients have the same sign as predicted by Equation 7 and they are exceptionally large.

The small thickness of the tube wall also makes it possible to use electric field-biased electrostrictive materials for the actuator application, since only a small bias voltage is required here to induce substantial piezoelectric responses in the materials. In field-biased electrostrictive materials, it has been shown that the ratio of the piezoelectric constants d_{33}/d_{31} is bias field-dependent [8]. Hence, for a suitable ratio R_0/r_0, by tuning the d.c. bias field level, both sign and magnitude of d_{31}^{eff} of the tube can be varied.

3. The hydrostatic response of end-capped tubes

The availability of small-sized ceramic tubes makes it attractive to integrate them into 1–3 type piezoceramic–polymer composites for large-area applications and to provide more flexibility for further material property modification. Before a detailed discussion on the composite properties, we will derive the expression for the hydrostatic response of end-capped tubes in this section since this is the most commonly used mode of piezo-tubes as hydrostatic sensors [9, 10]. Again here, the ratio R_0/r_0 provides a convenient way to adjust the piezoelectric response of the sensor in the radial direction.

Similar to the derivations presented in the preceding section, the displacement field of a tube under hydrostatic pressure, when expressed in the cylindrical coordinate system, is $u_\phi = 0$ and $\boldsymbol{u} = u_r(r)\hat{r} + u_z(z)\hat{z}$. (For an isotropic material, this is the exact form of the displacement field and for a poled ceramic tube, the error in using this form of the displacement field, as will be shown later, is less than 10%.) Since all the external forces are applied on the surfaces of the tube, there is no internal body force in the tube wall and Equation 2 becomes

$$\frac{1}{r}\left(\frac{\partial(ru_r)}{\partial r}\right) = \text{const.} \qquad \frac{\partial u_z}{\partial z} = \text{const.} \tag{8}$$

The solutions to the equations are

$$u_r = ar + \frac{b}{r} \qquad u_z = cz \tag{9}$$

The non-zero strain components are

$$u_{rr} = a - \frac{b}{r^2} \qquad u_{\phi\phi} = a + \frac{b}{r^2} \qquad u_{zz} = c \tag{10}$$

where a, b and c are the integration constants. The boundary conditions which will be used to determine them are: since the two ends of the tube are sealed, there is no pressure inside the tube and at $r = r_0$, $T_r = 0$; at $r = R_0$, $T_r = -p$; and at $z = 0$ and $z = 1$, the stress in the axial direction is $T_z = -pR_0^2/(R_0^2 - r_0^2)$, where $-p$ is the applied hydrostatic pressure. For the purpose of comparison, we will determine the integration constants a, b and c in Equation 9 for both elastically isotropic tubes and anisotropic tubes. For the anisotropic tube, the constitutive relations are

$$\begin{aligned} T_z &= c_{11}u_{zz} + c_{12}u_{\phi\phi} + c_{13}u_{rr} \\ T_r &= c_{33}u_{rr} + c_{13}u_{\phi\phi} + c_{13}u_{zz} \\ T_\phi &= c_{12}u_{zz} + c_{11}u_{\phi\phi} + c_{13}u_{rr} \end{aligned} \tag{11}$$

where c_{ij} are the elastic stiffness coefficients of the poled ceramics. Following the convention in the literature, in Equation 11, 3 is referred to the poling direction ($\hat{r}$ direction), 1 the $\hat{z}$ direction, and 2 the $\hat{\phi}$ direction. Substituting the strain components in Equation 10 into Equation 11 and omitting the term in T_z having r dependence, one can obtain a, b, c:

$$a = \frac{-pR_0^2}{R_0^2 - r_0^2}\left(\frac{c_{13} - c_{11}}{c_{13}(c_{12} + c_{13}) - c_{11}(c_{13} + c_{33})}\right) \tag{12a}$$

$$b = \frac{-r_0^2R_0^2}{R_0^2 - r_0^2}\left(\frac{p}{c_{33} - c_{13}}\right) \tag{12b}$$

$$c = \frac{-pR_0^2}{R_0^2 - r_0^2}\left(\frac{c_{12} - c_{33}}{c_{13}(c_{12} + c_{13}) - c_{11}(c_{13} + c_{33})}\right) \tag{12c}$$

Therefore, the stress distribution in the tube is given by

$$T_r = \frac{-pR_0^2}{R_0^2 - r_0^2}\left(1 - \frac{r_0^2}{r^2}\right) \tag{13a}$$

$$T_\phi = \frac{-pR_0^2}{R_0^2 - r_0^2}\left[\frac{c_{13}^2 + c_{12}^2 - c_{11}^2 - c_{12}c_{33}}{c_{13}(c_{12} + c_{13}) - c_{11}(c_{13} + c_{33})} + \frac{c_{11} - c_{13}}{c_{33} - c_{13}}\left(\frac{r_0^2}{r^2}\right)\right] \tag{13b}$$

$$T_z = \frac{-pR_0^2}{R_0^2 - r_0^2} \tag{13c}$$

In writing down Equation 13c, we omitted a term $(c_{12} - c_{13})b/r^2$, which is less than 7% of the total T_z. Since T_z itself is one of the boundary condition used to derive the integration constants a, b and c and is equal to $-pR_0^2/(R_0^2 - r_0^2)$, the appearance of this extra term in the expression for T_z derived using Equations 11 and 12 is clearly unphysical and is the error resulted from the approximation made regarding the displacement field for the tube under hydrostatic pressure.

However, the small size of this error (less than 7%) indicates the validity of this approximation.

From the stress distribution equations, the hydrostatic response of the tube can be calculated from the relation

$$D_3 = d_{31}T_z + d_{31}T_\phi + d_{33}T_r \qquad (14)$$

where D_3 is the electric displacement in the poling direction. The value of the hydrostatic piezoelectric constant d_h can be found by taking the average charge produced in the inner and outer surfaces of the tube wall and dividing it by the outer surface area of the tube. This yields, from Equation 14,

$$d_h = \frac{1}{2}\left\{d_{33} + \frac{R_0}{R_0 - r_0} \times \left[1 + \left(\frac{c_{13}^2 + c_{12}^2 - c_{11}^2 - c_{12}c_{33}}{c_{13}(c_{13} + c_{12}) - c_{11}(c_{13} + c_{33})}\right) + \frac{c_{11} - c_{13}}{c_{33} - c_{13}}\left(\frac{r_0}{R_0}\right)\right]d_{31}\right\} \qquad (15)$$

In Equation 15, we have taken the tube outer surface as the total electroded area to calculate d_h. Using the elastic stiffness coefficients for PZT-5H [7], for a tube with $R_0 = 0.635$ mm and $r_0 = 0.381$ mm, Equation 15 predicts $d_h = -657\,\mathrm{pC\,N^{-1}}$ or $2.4d_{31}$. If the tube R_0 is doubled while keeping the wall thickness the same, the d_h value can reach $-1786\,\mathrm{pC\,N^{-1}}$. Hence, for thin-walled tubes, an exceptionally large hydrostatic response can be achieved.

Equation 13 can be reduced to the stress field of an elastically isotropic tube by using the isotropic conditions $c_{11} = c_{33}$, $c_{12} = c_{13}$. It can be shown that the result thus obtained is the exact solution to the tube stress field, and similarly d_h can be found by simplifying Equation 15 using the isotropic condition

$$d_h = \frac{1}{2}\left[d_{33} + \frac{R_0}{R_0 - r_0}\left(2 + \frac{r_0}{R_0}\right)d_{31}\right] \qquad (16)$$

For the PZT-5H tube just calculated, the calculated d_h value is $-594\,\mathrm{pC\,N^{-1}}$ $(2.17d_{31})$ when Equation 16 is used.

Experimental measurements were performance on several PZT-5 tubes ($R_0 = 0.635$ mm and $r_0 = 0.381$ mm) with two ends sealed and radially poled (the dielectric constant ε for this group of sample is around 1700 at atmospheric pressure). d_h was measured through the direct piezoelectric effect, where the charge induced on the electrodes of a sample is measured when the sample is subjected to a hydrostatic pressure. d_{31} and d_{33} were measured using a double-beam laser interferometer [6]. For this group of samples, d_h was in the range from -330 to $-400\,\mathrm{pC\,N^{-1}}$ and d_{31} from -140 to $-160\,\mathrm{pC\,N^{-1}}$. The ratio between the experimentally measured d_h and d_{31} (on average) is 2.45, which is very close to that predicted from Equation 15. Clearly, to make a quantitative prediction about the hydrostatic response of a tubular structure, one may be required to include the elastic anisotropy in the calculation.

By analogy with the situation discussed in the preceding section, by varying the ratio of R_0/r_0 one can also manipulate the response of the tube to the stress field in the radial direction. Here, we will use the result just derived for the hydrostatic response of a tube as an example. In Equation 14, the hydrostatic response of a tube comes from three terms: one is from the pressure in the axial direction and the other two from the pressure in the radial direction. The electric displacement D_3^r due to the pressure in the radial direction is

$$D_3^r = d_{31}T_\phi + d_{33}T_r$$

Using the result of Equation (13) and taking the average charge produced at the tube inner wall and outer wall, one can obtain the partial piezoelectric response d^r of the tube to the pressure in the radial direction

$$d^r = \frac{1}{2}\left\{d_{33} + \frac{R_0}{R_0 - r_0} \times \left[\left(\frac{c_{13}^2 + c_{12}^2 - c_{11}^2 - c_{12}c_{33}}{c_{13}(c_{13} + c_{12}) - c_{11}(c_{13} + c_{33})}\right) + \frac{c_{11} - c_{13}}{c_{33} - c_{13}}\left(\frac{r_0}{R_0}\right)\right]d_{31}\right\} \qquad (17)$$

Obviously, the opposite sign of d_{33} and d_{31} provides a convenient way to change d^r in Equation 17. One can easily verify that by varying the ratio R_0/r_0, d^r changes continuously from positive to zero, and to negative. Taking the elastically isotropic tube as an example and assuming $d_{33}/d_{31} = 2.2$ in Equation 17, when $r_0/R_0 = 0.375$, d^r becomes zero. That is, the tube now becomes insensitive to the pressure wave in the radial direction. Similar to the actuator case, for suitable ratio of r_0/R_0, one can also change the sign of the effective radial response here by using electrostrictive materials with different d.c. bias field levels. This result, as well as the result in the preceding section, indicates that the range of the effective piezoelectric properties of the materials can be considerably broadened by using tubular structures.

To calculate the hydrostatic figure of merit $d_h g_h$ for this tubular sensor, we notice that in practice, the quantity is a measure of the product of the charge and voltage produced in unit volume of material. For a tubular material its effective volume is $\pi R_0^2 L$, where L is the tube length when the end-capped tube is regarded as a rod with its radius equal to R_0. The capacitance of the tube is

$$C = \frac{2\pi L\varepsilon_0\varepsilon}{\ln(R_0/r_0)}$$

where ε is the dielectric constant of the material. Since the total charge produced by the tube is equal to $2\pi R_0 L d_h$ and the voltage is equal to this charge divided by the capacitance of the tube, the effective figure of merit for the tube is

$$d_h g_h = \frac{1}{2\varepsilon\varepsilon_0}\ln\left(\frac{R_0}{r_0}\right) \times \left[d_{33} + d_{31}\left(\frac{R_0}{R_0 - r_0}\right)\left(2 + \frac{r_0}{R_0}\right)\right]^2 \qquad (18)$$

Here, we have used the d_h result for an isotropic tube (Equation 17). One can easily expand the result to elastically anisotropic materials. Clearly, for a thin-walled tube a large figure of merit can be obtained.

4. 1–3 tubular composites

A typical 1–3 tubular composite is schematically drawn in Fig. 2. For the composite discussed here, the tubes are radially poled and the composite is electroded on the two end-faces. Hence, a special arrangement is required to ensure proper electric connections between the electrodes at the tube walls and the composite end-faces. This kind of composite can be used for large-area actuator and sensor applications, as well as "smart" materials where both sensor and actuator are integrated into one structure. In this section, we only discuss the properties associated with sensor applications.

When tubes are integrated into a 1–3 type ceramic–polymer composite, as has been demonstrated in our earlier publications, there is a stress transfer between the polymer matrix and the ceramic tubes in the z direction [11, 12]. This stress transfer is a result of the difference in the elastic constants between the two constituent phases and is through the shear force in the two phases. Due to this stress transfer, the piezoelectric response of the tube in the axial direction is enhanced. To provide a physical picture of how the hydrostatic response of a tubular 1–3 composite changes as the elastic properties of the two constituent phases and their geometric parameters are varied, we will treat quantitatively the composite schematically drawn in Fig. 3. This composite corresponds to the tubular composite in the dilute limit. However, since only the polymer matrix close to the ceramic–polymer interface participates the stress transfer, the result can also be applied to the composite with finite ceramic content.

The procedure of calculating how much stress is transferred from the polymer phase to the ceramic rod

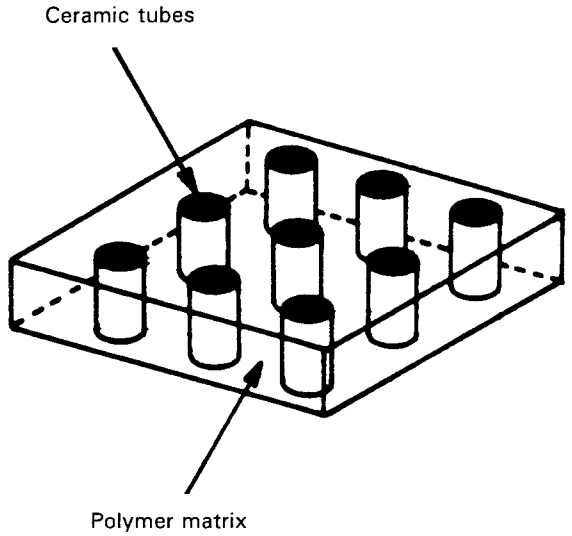

Figure 2 Schematic drawing of 1–3 tubular composite where the ceramic tubes are embedded in a polymer matrix. The ceramic tubes are either end-capped or filled inside with epoxy.

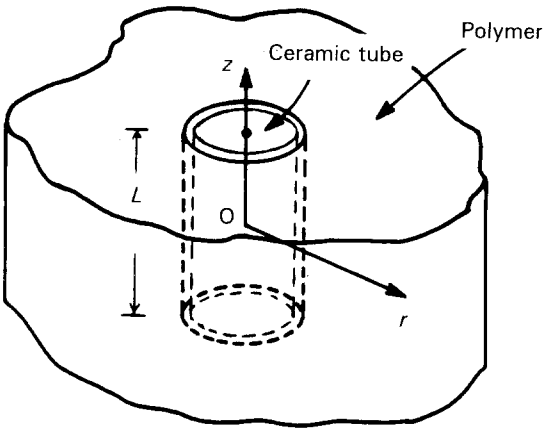

Figure 3 A single tube 1–3 composite. The ceramic tube is end-capped.

is similar to that outlined in the earlier publications. [11, 12]. Under hydrostatic pressure p, the surface displacement field u_z of the polymer phase in the z direction should satisfy the equation

$$\frac{2u_z}{L} = -(s_{11} + 2s_{12})p + \frac{s_{11}\mu L}{4}\left[\frac{\partial^2 u_z}{\partial r^2} + \frac{1}{r}\left(\frac{\partial u_z}{\partial r}\right)\right] \quad (19)$$

where p is the hydrostatic pressure, s_{ij} is the elastic compliance of the polymer phase, μ is the shear modulus of the polymer phase, and L is the thickness of the composite in the z direction. The solution to Equation 19 is the zero-order Hankel function $K_0(\rho)$ and

$$\frac{2u_z}{L} = -\frac{(1 - 2\sigma)p}{Y} + AK_0(r/\xi) \quad (20)$$

where A is the integration constant and $\xi = L/[2(2Y/\mu)^{1/2}]$ defines the strain decay length in the polymer phase. In Equation 20 we have made use of the relations $s_{12} = -\sigma s_{11}$ and $Y = 1/s_{11}$, where Y and σ are the Young's modulus and Poisson's ratio of the polymer, respectively. The total force f transferred from the polymer phase to the ceramic tube is therefore

$$f = -Y\int_{R_0}^{\infty} 2\pi r A K_0(r/\xi)\,dr$$

Two boundary conditions are needed to determine f. The first one is the boundary condition that at the ceramic tube–polymer interface, the z component of the strain in the two phases should be equal, and the second is the relation between the z component of the strain in the ceramic tube and the stress field

$$u_{zz} = -\frac{pR_0^2(1 - 2\sigma^c)s_{11}^c}{R_0^2 - r_0^2} + \frac{fs_{11}^c}{\pi(R_0^2 - r_0^2)} \quad (21)$$

where s_{11}^c and σ^c are the elastic compliance and Poisson's ratio of the ceramic tube, respectively. Equation 21 can be derived by following the procedure outlined in the preceding section. Hence, the amount of stress transferred from the polymer matrix to the

ceramic tube is

$$\frac{f}{\pi A_0} = -\frac{pR_0^2}{A_0}\left(\frac{A_0(1-2\sigma)/(R_0^2 Ys_{11}^c) - (1-2\sigma^c)}{1 + K_0(\rho_0)A_0/[2K_1(\rho_0)Ys_{11}^c R_0\xi]}\right) \tag{22}$$

where $A_0 = (R_0^2 - r_0^2)$, $\rho_0 = R_0/\xi$ and $K_1(\rho)$ is the first-order Hankel function. Since the polymer phase is subjected to a hydrostatic pressure, the Poisson's ratio effect causes a reduction of the effective pressure at the polymer faces from $-p$ to $-p(1-2\sigma)$. As shown in Equation 22, this reduces the stress transfer from the polymer phase to the ceramic tube. To increase the stress transfer, one should choose polymers with a small Poisson's ratio. The total stress in the axial direction of the tube is

$$T_z = -\frac{pR_0^2}{A_0}\left(1 + \frac{A_0(1-2\sigma)/(R_0^2 Ys_{11}^c) - (1-2\sigma^c)}{1 + K_0(\rho_0)A_0/[2K_1(\rho_0)Ys_{11}^c R_0\xi]}\right)$$

$$T_z = -\frac{pR_0^2}{A_0}\gamma \tag{23}$$

where γ is introduced as the stress amplification factor. In Fig. 4 we plot γ as a function of the aspect ratio R_0/L for a 1–3 tubular composite made of PZT-5H tube with $R_0 = 0.635$ mm and $r_0 = 0.381$ mm and Spurrs epoxy. The data used are: $Y = 3.1\ (10^9\ \mathrm{N\,m^{-2}})$, $\mu = 1.148\ (10^9\ \mathrm{N\,m^{-2}})$, and $\sigma = 0.35$ for spurs epoxy (from Oakley [13]; $s_{11}^c = 1.64\ (10^{-11}\ \mathrm{m^2\,N^{-1}})$ and $\sigma = 0.31$ [7]. Apparently, for thin and long tubes, the stress amplication factor is large. This is similar to that obtained earlier for 1–3 composites made of ceramic rods [11, 12].

Using the results from section 3 and Equation 23, one can write down the effective hydrostatic piezoelectric strain coefficient for 1–3 tubular composites as

$$d_h^{\mathrm{eff}} = \frac{L}{R_0}v_c\left[d_{33} + \frac{R_0}{R_0 - r_0}\left(1 + \gamma + \frac{r_0}{R_0}\right)d_{31}\right] \tag{24}$$

where v_c is the volume content of ceramic tubes in the composite which is defined as $v_c = \pi R_0^2/a$, and a is the unit cell area of the composite. For a composite of low ceramic volume content, γ in Equation 22 is equal to that in Equation 24. With increased volume content, the dependence of γ on the material properties of the constituent phases will become more complicated and one may not be able to derive the analytical expression for γ except in some special cases. In this paper, we will not pursue this further and only point out that in the composite, there is always a stress transfer between the two phases ($\gamma > 1$); the general rule to increase this stress transfer is basically the same as that for the dilute composite case.

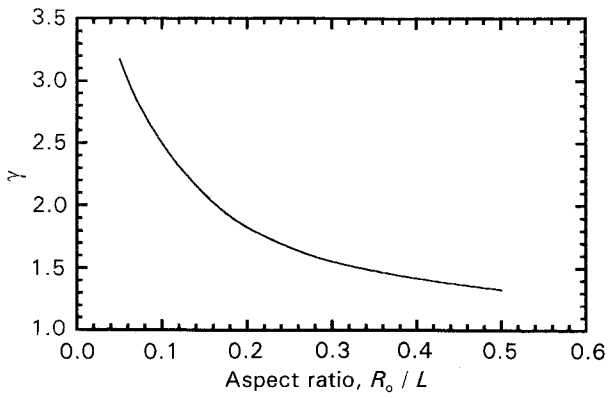

Figure 4 The stress amplification factor γ (Equation 23) as a function of the aspect ratio R_0/L of the ceramic tube for the composite drawn in Fig. 3 with PZT-5H ceramic tube and spurs epoxy.

In the limit of $v_c \to 1$, Equation 24 is reduced to that for a single tube when regarded as a rod with similar dimensions:

$$d_h^{\mathrm{eff}} = \frac{L}{R_0}\left[d_{33} + \frac{R_0}{R_0 - r_0}\left(2 + \frac{r_0}{R_0}\right)d_{31}\right] \tag{25}$$

Equation 16 can be converted to Equation 25 by using the area of the tube end (πR_0^2) as the effective electrode area instead of the area of the tube outer wall. Similarly, one can also derive the effective hydrostatic figure of merit for 1–3 tubular composites as

$$d_h^{\mathrm{eff}} g_h^{\mathrm{eff}} = \frac{V_c}{2\varepsilon\varepsilon_0}\ln\left(\frac{R_0}{r_0}\right) \times \left[d_{33} + \frac{R_0}{R_0 - r_0}\left(1 + \frac{r_0}{R_0} + \gamma\right)d_{31}\right]^2 \tag{26}$$

As $v_c \to 1$ ($\gamma \to 1$), the result is reduced to that for a single tube sensor (Equation 18).

For comparison, in Table I we present the experimental values of the hydrostatic response of an end-capped ceramic tube, a 1–3 composite with tubes having inside air backing, and a 1–3 composite with tubes having inside epoxy backing. All 1–3 composites had a volume content of 23.3% ceramic tube and the dimensions of the tubes are $R_0 = 0.635$ mm, $r_0 = 0.381$ mm and $L = 9$ mm. The polymer matrix was made of spurs epoxy. In the composite with epoxy backing, the tube inside was filled with Spurrs epoxy. d_{31} listed in the table was calculated using Equation 25 where the ratio $d_{33}/d_{31} = 2.2$ is used. From this d_{31}, γ was calculated from Equation 26. Clearly, the γ value here is much smaller than that shown in Fig. 4 ($R_0/L = 0.07$ here). One of the reasons for this is that Fig. 4 is for the composite in the dilute limit; the γ value for composites with a finite ceramic content should be smaller than that in Fig. 4. The imperfect stress transfer between the two phases and the depoling effect of the tubes during epoxy curing may also be responsible for this reduction of γ. Although the data in Table I show that the hydrostatic responses of the composites tested are not as high as that of the single tube, the difference is not very large. As the volume content of the ceramic tube and other parameters in a composite are varied, the effective hydrostatic figure of merit for 1–3 tubular composites will change. In the optimum condition, one would expect that $d_h^{\mathrm{eff}} g_h^{\mathrm{eff}}$ for a tubular 1–3 composite may exceed that of a single tube. Apparently, further experimental and theoretical work is required to address this issue. Furthermore,

TABLE I Hydrostatic properties of the end-capped tube and 1–3 tubular composites

	ε	d_h^{eff} ($pC\,N^{-1}$)	$d_h^{eff} g_h^{eff}$ ($10^{-15}\,m^2\,N^{-1}$)	d_{31} ($pC\,N^{-1}$)	γ
End-capped tube	2945	− 14330	10000	− 235	1
Composite					
Air backing	2922	− 5502	6389	− 235	2.11
Epoxy backing	2944	− 4970	5172	− 235	

the figure of merit of 1–3 tubular composites is much higher than that of 1–3 composites made of ceramic rods [12].

If there was no stress transfer from the polymer phase to the ceramic tubes in these tubular composites, one would get for this 1–3 composite $d_h^{eff} = 3339\,pC\,N^{-1}$ and $d_h^{eff} g_h^{eff} = 2353 \times 10^{-15}\,m^2\,N^{-1}$, which are much smaller than the values listed in Table I. This clearly demonstrates the importance of the stress transfer between the two phases in a 1–3 composite.

One interesting feature from Table I is that the hydrostatic response of the 1–3 tubular composite with epoxy backing does not differ very much from that with air backing. That is, the epoxy filling inside a tube does not change the stress distribution in the tube wall significantly except to transfer stress in the z direction. This can be understood by considering the following fact: the elastic moduli of the ceramic tube are much higher than those of epoxy, and as a result the ceramic tube wall practically shields the epoxy filling inside the tube from seeing the pressure in the radial direction. Conversely, the epoxy inside the tube does not exert a significant amount of stress on the ceramic tube wall in the radial direction. Therefore, the epoxy filling inside a tube provides an effective way to enhance the mechanical strength while keeping the hydrostatic response of the composite almost intact.

5. Summary

In this paper, the effective piezoelectric responses of the tubular structure and its composites were evaluated both theoretically and experimentally. When used as actuators, the effective piezoelectric constant in the radial direction of a tube can be changed from positive to zero and to negative by adjusting the ratio R_0/r_0 for piezoelectric materials or the d.c. bias field for electrostrictive materials. Therefore, the effective piezoelectric constants along the axial direction and the radial direction can both have the same sign. For sensor applications, the tube with two ends sealed exhibits an exceptionally high hydrostatic response and, analogous to the situation with actuators, the pressure response in the radial direction can be adjusted by the ratio R_0/r_0 for piezoelectric materials or the d.c. bias field for the electrostrictive materials. For large-area applications, these tubes can be readily integrated into a 1–3 composite structure which provides a low acoustic density and high piezoelectric activity. The effectiveness of the stress transfer between the polymer phase and the ceramic tube in a 1–3 composite makes it possible to back-fill the inside of the ceramic tube, which increases the mechanical integrity of the tubular structure while keeping the piezoelectric response of the composite almost intact.

Acknowledgements

The authors wish to thank Dr J. Powers for many stimulating discussions. The technical assistance of Mr H. Chen is greatly appreciated. This work was supported by the Office of Naval Research.

References

1. R. E. NEWNHAM and G. R. RUSCHAN, *J. Amer. Ceram. Soc.* **74** (1991) 463.
2. R. E. NEWNHAM, Q. C. XU, S. KUMAR and L. E. CROSS, *Ferro.* **102** (1990) 259.
3. R. E. NEWNHAM, D. P. SKINNER and L. E. CROSS, *Mater. Res. Bull.* **13** (1978) 525.
4. W. A. SMITH, in Proceedings of 1990 IEEE International Symposium on Appl. of Ferro., (Urbana, Illinois, 1990) p. 145.
5. L. D. LANDAU and E. M. LIFSHITZ, "Theory of Elasticity" (Pergamon, 1986).
6. Q. M. ZHANG, S. J. JANG and L. E. CROSS, *J. Appl. Phys.* **65** (1989) 2807.
7. PZT-5 data sheet, 1991 (Morgon Matroc, Inc., Vernitron Division, OH).
8. D. J. TAYLOR, D. DAMJANOVIC, A. S. BHALLA and L. E. CROSS, in Annual Report of the Materials Research Laboratory (The Pennsylvania State University, University Park, PA, 1991) p. 50.
9. R. A. LANGEVIN, *J. Acoust. Soc. Amer.* **26** (1954) 421.
10. "Handbook of Hydrophone Element Design Technology", NUSC Technical Document 5813 (1978).
11. Q. M. ZHANG, WENWU CAO, H. WANG and L. E. CROSS, *J. Appl. Phys.* **73** (1993) 1403.
12. WENWU CAO, Q. M. ZHANG and L. E. CROSS, *ibid.* **72** (1992) 5814.
13. C. G. OAKLEY, PhD Thesis, The Pennsylvania State University (1991).

Received 23 November
and accepted 8 December 1992